Extension of Torsionally Stressed DNA by External Force

Alexander V. Vologodskii* and John F. Marko#
*Department of Chemistry, New York University, New York, New York 10003, and #Department of Physics, The University of Illinois at Chicago, Chicago, Illinois 60607-7059 USA

ABSTRACT Metropolis Monte Carlo simulation was used to study the elasticity of torsionally stressed double-helical DNA. Equilibrium distributions of DNA conformations for different values of linking deficit, external force, and ionic conditions were simulated using the discrete wormlike chain model. Ionic conditions were specified in terms of DNA effective diameter, i.e., hard-core radius of the model chain. The simulations show that entropic elasticity of the double helix depends on how much it is twisted. For low amounts of twisting (less than about one turn per twist persistence length) the force versus extension is nearly the same as in the completely torsionally relaxed case. For more twisting than this, the molecule starts to supercoil, and there is an increase in the force needed to realize a given extension. For sufficiently large amounts of twist, the entire chain is plectonemically supercoiled at low extensions; a finite force must be applied to obtain any extension at all in this regime. The simulation results agree well with the results of recent micromanipulation experiments.

INTRODUCTION

Rapid development of micromanipulation methods over the past few years has made possible precise mechanical studies of individual DNA molecules (Smith et al., 1992, 1996; Perkins et al., 1994, 1995; Cluzel et al., 1996; Strick et al., 1996). These techniques present opportunities to improve our understanding of DNA. At the same time, analysis of experiments on individual DNAs has opened up new theoretical problems. The now-classic study of DNA elasticity by Smith et al. (1992) is a good example of this interplay of experiment and theory. Analysis of the measured force-extension dependence in terms of the freely joined model of a polymer chain showed a large discrepancy between theoretical and experimental results for high extensions. The reason for the discrepancy became clear only after quantitative analysis of the extension in terms of the wormlike chain model (Bustamante et al., 1994; Vologodskii, 1994; Marko and Siggia, 1995a). Comparison of the experimental data with the theoretical treatment of the wormlike chain extension showed remarkably good agreement and allowed definitive measurement of the DNA persistence length at low salt concentrations. Theoretical analysis of the more complex situation of the elasticity of DNA that is torsionally stressed, or twisted, is the subject of this paper.

The entropic elasticity of twisted DNA is of biophysical importance for two reasons. First, the elasticity of the double helix affects how it is manipulated in the cell: the double helix is bent and twisted during its transcription and replication. Second, large DNA molecules are often closed into "loops" of fixed topology (e.g., plasmids, chromosomal domains); double-helix elasticity determines how such a loop will supercoil in response to changes in its topology. The bending persistence length and the torsional rigidity C are the basic physical quantities related to these issues.

One of the aims of our study is the determinination of C via comparison with experiment. Measurement of C by direct micromanipulation is motivated by the lack of consensus between other indirect measurements (see reviews by Hagerman, 1988; Crothers et al., 1992). Further motivation for micromanipulation experiments is that they allow much larger twist strains to be applied to DNA than is possible by biochemical means, and should allow precise study of the breakdown of linear DNA elasticity (i.e., its description in terms of persistence length and C) and stress-induced changes in DNA structure.

Techniques for the measurement of entropic elasticity of large single DNA molecules have been developed in several laboratories (Smith et al., 1992; Cluzel et al., 1996; Smith et al., 1996). These experiments exploit the specificity of DNA's base pairing to make single-stranded attachments of DNAs to microscope slides and magnetic beads. Application of a force to the movable bead (using a magnetic field or a flow) allows a tensile stress to be put on the molecule. However, DNA can swivel around the single bonds in single-stranded attachments, eliminating the possibility of applying twist to the molecule if only one strand is anchored. Both strands must be anchored at both ends of the molecule to study its elasticity as a function of twisting.

A method to anchor both strands has been developed by two groups (Cluzel et al., 1996; Strick et al., 1996), exploiting the fact that linear λ-DNAs have short, complementary single-stranded ends. Linear λ-DNA is randomly labeled with biotin or digoxigenin every few hundred base pairs, and is then cut with a restriction enzyme. The labeled end fragments (4 kb to 6 kb) can then be attached, using the single-stranded ends, to other, unlabeled λ-DNAs. The resulting constructs then can be stuck to a bead or surface coated with streptavidin or anti-digoxigenin; if more than

Received for publication 6 January 1997 and in final form 26 March 1997.
Address reprint requests to Dr. Alex Vologodski, Department of Chemistry, New York University, 29 Washington Place, New York, NY 10003. Tel.: 212-998-3599; Fax: 212-260-7905; E-mail: avologod@jethro.cs.nyu.edu.

0006-3495/97/07/123/10 $2.00

one attachment is made at each end, the DNA is torsionally immobilized.

In the experiments of Strick et al. (1996), one end of a λ-DNA (~50 kb) was attached to a microscope slide, while the other end was attached to a magnetic bead. A magnetic field pointing in the plane of the microscope slide was applied to fix the orientation of the bead. Rotation of the magnet poles thus turned the bead (the torque applied to the bead was far greater than the torque applied by the twisted DNA, so the total rotation angle was held fixed). The gradient of the magnetic field in the direction perpendicular to the microscope slide applied a force to the bead. Thus Strick et al. were able to independently control the twisting and the tension applied to a DNA. They then measured the extension of their molecules in the direction perpendicular to the slide, using the beads to locate the free end of the DNA.

If one considers the anchoring points to be on impenetrable walls, the topological linking number Lk of the double helix is fixed in the experiment of Strick et al. (1996). That experiment therefore measured the entropic elasticity of the double helix, subject to the constraint of fixed Lk. In this paper we treat this problem by numerical Monte Carlo (MC) methods. The DNA is taken to be an elastic rod, with bending elasticity and twisting elasticity. The constraint of fixed Lk is applied by the use of the familiar White formula, $Lk = Tw + Wr$ (White, 1969; Fuller, 1971), whereby the twisting energy may be expressed in terms of linkage, Lk, and the writhe, Wr, of the DNA between the attachment points (Hao and Olson, 1989; Klenin et al., 1991). Some care must be taken when generalizing this formula to the case of a linear molecule; this is discussed when we present our model in the next section.

The results of our study are presented in the third section. We find that for low torsional stress, the force versus extension is nearly the same as for no such stress at all. This is reasonable, because in this regime, thermally excited twist and writhe overwhelm the externally introduced linkage. However, for larger amounts of torsional stress, the force needed to obtain a given extension is increased. Finally, for large enough torsional stress, the molecule is fully supercoiled if no tension is applied. In this last situation, a finite force must be applied to achieve any extension at all, corresponding to the fact that the plectonemic supercoils require work to be done on them to be converted into extended DNA. In the fourth section we compare our results to the experimental data of Strick et al. (1996).

MODEL AND METHODS OF COMPUTATIONS

The model

We used the discrete wormlike chain model introduced earlier for computer simulation of DNA (Frank-Kamenetskii et al., 1985; Klenin et al., 1989; Vologodskii et al., 1992; Vologodskii, 1994). A polymer chain composed of n Kuhn statistical segments was modeled as a chain consisting of mn rigid straight segments of equal size. The elastic energy of the chain, E_b, was calculated as

$$E_b = kT\alpha \sum_{i=1}^{mn-1} \theta_i^2 \qquad (1)$$

where the summation is over all of the joints between the rigid segments, α is the bending rigidity constant, and θ_i is the angular displacement of segment i relative to segment $i - 1$. The bending rigidity constant α is defined so that the Kuhn statistical length corresponds to m rigid segments (Frank-Kamenetskii et al., 1985). This model becomes the wormlike chain model as m approaches infinity. It has previously been shown that even for a highly supercoiled DNA molecule, simulated properties do not depend on m if it exceeds 10 (Vologodskii et al., 1992). Therefore, $m = 10$ was used in the current work, for which the bending constant $\alpha = 2.403$.

The chain was restricted by two impenetrable parallel walls crossing the chain ends (Fig. 1). The walls were always parallel to the yz plane and thus were perpendicular to the direction of the force (x) applied to the chain ends. Although these walls created entropic repulsion for low chain extensions, this effect was small for extensions larger than 0.25 of the chain contour length. The walls play the role of the magnetic bead and the surface to which the chain is attached in the experimental system; they also greatly simplify unambiguous calculation of the chain writhe, Wr (see below).

We assumed that torsional energy, E_t, is a quadratic function of the displacement of the chain twist from equilibrium, ΔTw, and is independent of the DNA bending:

$$E_t = (2\pi^2 C/L)(\Delta Tw)^2 \qquad (2)$$

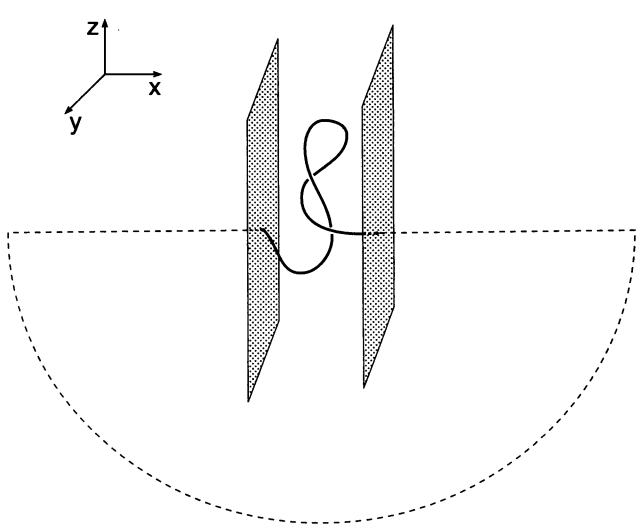

FIGURE 1 Diagram of the model chain used in the simulations. Conformations of basic chain, which is shown by a solid line, were restricted by two parallel walls attached to chain ends. The dashed line shows a part of the contour that was added to close the basic chain.

where C is the torsional rigidity constant and L is the DNA length. Available data support the assumption of harmonic twist elasticity (Vologodskii and Cozzarelli, 1993). We did not compute ΔTw directly because Tw was not specified in our model. Instead, we used the equation (White, 1969; Fuller, 1971)

$$\Delta Tw = \Delta Lk - Wr \tag{3}$$

where writhe, Wr, is a property of the chain axis alone, and linking number difference, ΔLk, was a parameter of a simulation run. This approach allows much faster computations in comparison with approaches based on explicit specification of Tw of each segment (Tan and Harvey, 1989; Katritch and Vologodskii, 1996). However, use of Eq. 3 in our case is complicated because ΔLk and Wr are not defined for a linear chain.

To solve this problem, we simply added long straight "sticks" to our DNA, allowing the chain to be considered to be "virtually closed" at infinity (Fig. 1). If the virtual closure is not supposed to contribute to the value of Tw, then the value of ΔLk is simply equal to the number of turns introduced by the rotation of the chain end (i.e., rotation of the experimental bead). As expected, we found that the contribution to Wr from the interaction of the closure path with the basic chain is small, typically $\sim 1\%$ of the basic chain Wr. For most of the simulations we used only two extra segments at each end of the chain to calculate Wr, which was then substituted into Eq. 3.

It should be emphasized that although Eqs. 2 and 3 correspond to the energy of uniform distribution of the twist deformation along the DNA contour, they also exactly describe fluctuations in local twist, assuming a harmonic dependence of energy on the local twisting of the individual segments. This follows from the fact that fluctuations of local twist angles away from the net twist Tw contribute harmonic terms to the energy that are independent of Tw (to see this, simply expand the individual harmonic degrees of freedom around the state of uniform twist). The fluctuations can then be formally "summed over" and simply do not affect the statistics of the chain axis conformations (this initial summation contributes an exactly calculable Tw-independent constant to the free energy). The only part of the twist that affects the chain conformations is the net twist Tw, through Eqs. 2 and 3. This property of the harmonic twist energy model has been exploited for many years in MC simulations of DNA supercoiling (Klenin et al., 1989; Vologodskii et al., 1992; Vologodskii, 1994; Gebe et al., 1995); it is important to use this fact, as simulation of the harmonic twist fluctuations adds a needless and large computational burden. A formal proof of this property of the model was recently presented by Gebe et al. (1996).

The model also takes into account excluded volume interactions between the DNA segments. We incorporated these interactions into the model via the concept of the effective diameter, d, the actual diameter of the cylindrical segments of the model. Its value takes into account not only the physical diameter of DNA, but also the electrostatic repulsion between DNA segments. The effective diameter of DNA is defined as the diameter of an uncharged model chain that mimics the conformational properties of actual DNA. Its quantitative definition is based on the concept of the second coefficient of virial expansion (Stigter, 1977).

The simulation procedure

Equilibrium sets of chain conformations for different values of the force, f, and ΔLk were constructed using the Metropolis MC procedure (Metropolis et al., 1953). Two types of chain displacements were considered. In the first type, an internal subchain containing an arbitrary number of adjacent segments was rotated by a randomly chosen angle, ϕ^1, around the straight line connecting the two vertices bounding the subchain. In the second type, a subchain between a randomly chosen vertex and one of the free chain ends was rotated by a randomly chosen angle, ϕ^2, around a randomly oriented line passing through the vertex. Note that the first type of move cannot change the total end-to-end extension of the chain, thus necessitating the second type of move. The values of ϕ^1 and ϕ^2 were uniformly distributed over intervals $(-\phi_0^1, \phi_0^1)$ and $(-\phi_0^2, \phi_0^2)$, chosen so that about half of the proposed moves of each type were accepted.

To simulate the extension of the model chain, we fixed one of its ends at point 0 and applied a force, f, directed along the x axis, to the second end. The total energy for a particular conformation, E, was

$$E = E_b + E_t - fx \tag{4}$$

where x is the x-coordinate of the second end of the chain.

The Gauss integral was used in the calculation of the chain (see White, 1989, for example). For our discrete wormlike chain the integral is reduced to a double sum over chain segments (Vologodskii et al., 1979).

The starting conformations of the chain were unknotted. However, this does not guarantee that the chain will remain unknotted during Monte Carlo simulation, because segments of the chain were allowed to cross one another during trial moves. With such a "phantom" chain, knot-checking was necessary even for short chains, because supercoiling sharply increases the probability of knotting. Knots were detected by evaluating the Alexander polynomial $\Delta(t)$ for the trial conformation at $t = -1$ (Vologodskii et al., 1974). If a trial move knotted the chain, it was rejected. For some simulation runs we omitted this topology test to investigate its effect on the results.

Most of the calculations were done for model chains consisting of 10 Kuhn statistical segments, and most results were nearly the same for 20 segments (see below). To obtain equilibrium averages, up to 2×10^6 elementary displacements were produced for particular values of f and ΔLk.

In all simulations the persistence length a was taken to be 50 nm (Hagerman, 1988). The twist persistence length C/kT

was equal to 75 nm (torsional rigidity $C = 3 \times 10^{-19}$ erg·cm) for most of the runs; cases in which other values of the twist persistence length were used will be indicated below. We simulated DNA extension for two different concentrations of sodium ions, 0.2 M and 0.02 M, by setting the DNA effective (hard-core) diameter to 5 nm and 11 nm, respectively (Stigter, 1977; Brian et al., 1981; Rybenkov et al., 1993; Shaw and Wang, 1993). The temperature was assumed to be 300 K in all cases ($kT = 4 \times 10^{-14}$ erg).

RESULTS

Force versus extension at high salt concentration

It is known that different alternative DNA structures such as cruciforms, Z-form, open regions, and H-form appear in DNA under the stress of negative supercoiling (see Vologodskii, 1992, for a review). Negative supercoiling induces formation of these structures because they have a much lower linkage of the DNA complementary strands than regular B-DNA. This problem dramatically complicates quantitative analysis of the large-scale structure of highly supercoiled DNA. To avoid the problem, we considered in this paper extension of positively supercoiled DNA for which secondary structure does not change over a wide range of stress.

We first simulated extension of torsionally stressed linear molecules at high ionic conditions, where the excluded volume only slightly affects the simulation results. Fig. 2 shows force versus extension for superhelix density σ ranging from 0.00 to 0.05 ($\sigma = \Delta Lk/Lk_o$, where Lk_o is the equilibrium number of turns in the unstressed DNA). First of all, the figure shows that extension versus force dependences for our model are nearly independent of chain length if extension, $\langle x \rangle/L$, exceeds 0.4.

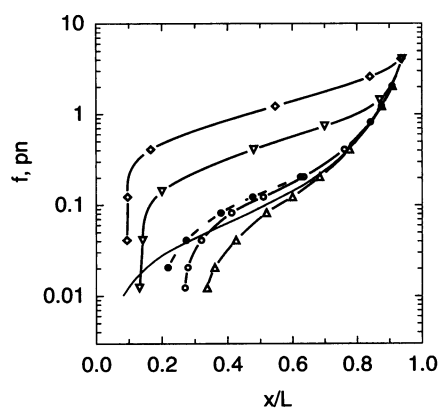

FIGURE 2 Simulated extension of torsionally stressed DNA under the action of force. Symbols show MC results for $\sigma = 0$ (△), 0.01 (○, ●), 0.03 (▽), and 0.05 (◇). Hard-core interactions mimic a monovalent salt concentration of 200 mM. Open symbols indicate results for chains of 10 Kuhn segments (corresponding to 1000-nm or 3-kb DNAs); black circles indicate results for 20 Kuhn segment chains with $\sigma = 0.01$. The statistical errors of the simulations are smaller than the symbols. At low forces, the extension saturates at a value greater than zero because of the impenetrable walls that confine the chain (see text and Fig. 1). The thin solid line indicates the result for $\sigma = 0$ for an infinite wormlike chain with no torsional constraint and a persistence length of 50 nm.

Extension in the absence of torsional stress

For $\sigma = 0$, the simulated chain has nearly the same force-distance behavior as the infinite wormlike chain for forces above 0.1 pN (see Fig. 2). Therefore, neither the finite chain length (10 Kuhn segments), nor the constraint of fixed (zero) σ, nor the finite hard-core diameter affects the entropic elasticity for chain extensions $\langle x \rangle/L > 0.5$. Each of those effects will remain small in that regime for long chains: the finite-chain effect diminishes exponentially with the chain length; fluctuations in σ (defined for an open chain as above) for long, torsionally unconstrained chains go to zero as the inverse of the square root of the chain length; for large extensions the chain rarely encounters itself, and thus the hard-core interactions are also unimportant (Vologodskii, 1994; Marko and Siggia, 1995a).

Note that for $\sigma = 0$, a 10 Kuhn segment chain has a finite extension $\langle x \rangle/L \approx 0.25$ at zero force, whereas the ideal wormlike chain extension goes linearly to zero as force goes to zero. This qualitative difference is caused by the impenetrable walls to which it is attached (recall from the first section above that those walls are essential to the definition of linking number for a linear chain). If zero force is applied to the chain ends, the requirement that the walls remain outside the chain forces the extension to remain at roughly the free chain radius. A negative (compressive) force would have to be applied to the walls to further reduce $\langle x \rangle/L$ to overcome the osmotic pressure exerted by the chain segments on the walls.

For a 10 Kuhn segment chain, we can thus expect an extension of at least 3 Kuhn segments (i.e., the random walk size), or $\langle x \rangle/L \approx 0.3$. This effect is to be expected experimentally (the DNAs in the experiment of Strick et al. are confined between a glass wall and a 3-μm-diameter bead), although for a large chain, $\langle x \rangle/L$ at zero force will diminish as $L^{-1/2}$. For a sufficiently long chain, self-avoidance will swell the chain, causing small deviations from ideal-chain behavior for low extensions (de Gennes, 1979).

Extension of twisted DNA

As σ is increased from zero, the force required to obtain a given extension increases. This is intuitively plausible because an increase in the linkage will cause the molecule to writhe. Full extension of the molecule moves the linkage from writhe into twist, and the work done during twisting must come from the applied force. Note that the force-distance curve becomes appreciably perturbed from the $\sigma = 0$ result only for $\sigma > 0.01$. Because this is the point at which one link has been inserted per $2\pi C/kT$, it is the point at which the excess linkage per twist persistence length is comparable to twist fluctuations. For $\sigma < 0.01$, the inserted linkage per length is dwarfed by random thermal twists of

the chain, so the entropic elasticity is essentially due to the wormlike-chain bending degrees of freedom.

For $\sigma > 0.01$, the force required to achieve a fixed extension quickly rises: for $\sigma \approx 0.05$, the force at half-extension is ~1 pN, a factor of 10 larger than the force required to half-extend the $\sigma = 0$ molecule. Note also that as σ is increased, the limiting extension for low forces less than 0.1 pN decreases; this limiting extension approaches zero as σ is increased. This reflects the writhing of the chains at low forces for $\sigma > 0.01$.

For $\sigma > 0.03$, the chains are predominantly plectonemically supercoiled at low extension, leading to a sharpening of the approach to the limiting $\langle x \rangle / L$ value for $\sigma > 0.03$. Analytical theory for the large-L limit predicts a sharp behavior $\langle x \rangle / L \approx f - f_0$ for some finite-threshold force f_0 when the molecule is fully plectonemically supercoiled at zero force. This threshold behavior reflects the finite work per length that must be done to convert the "bound" plectoneme into extended DNA (Marko and Siggia, 1994, 1995a; Marko, 1997).

The writhe *Wr*, as a function of force, for the cases $\sigma =$ 0.01, 0.03, and 0.05 (corresponding to $\Delta Lk = 2.8$, 8.4, and 14.0 turns, respectively, for ~10 Kuhn segment chain) is shown in Fig. 3. In each case, at low forces, *Wr* saturates at a value of ~0.7 ΔLk, in agreement with the *Wr* per ΔLk for closed circular DNAs (see Vologodskii and Cozzarelli, 1994a, for a review). When force is applied, the *Wr* decreases: for very large forces the molecule is forced to be extended, and *Wr* drops to zero. For $\sigma = 0.01$, the drop-off is rather gentle, occurring over the entire force range. In this case the molecule is a "chiral random coil" for low forces and can be smoothly extended with a gradual reduction of *Wr*.

For $\sigma = 0.03$, *Wr* is nearly constant up to 0.2 pN, and then abruptly drops to near zero by ~1 pN; for $\sigma = 0.05$, *Wr* is constant up to ~1 pN, and then at 3 pN has plummeted to nearly zero. Thus *Wr* has a sharper variation with force for $\sigma = 0.03$ and 0.05 than it did for $\sigma = 0.01$. This again reflects that for $\sigma > 0.03$, the chains are fully plectonemically supercoiled at zero force (Marko and Siggia, 1994, 1995a; Vologodskii and Cozzarelli, 1994a), and therefore a force threshold exists below which the molecule is essentially unperturbed. A sample configuration for $\sigma =$ 0.05 and $f = 0.2$ pN (Fig. 4) shows this clearly: the chain is nearly completely plectonemically supercoiled, with almost no extension of its ends (note that for $\sigma = 0$, $\langle x \rangle / L \approx 0.65$ for $f = 0.2$ pN). Of course, no single picture can indicate the "conformation" of these large, flexible molecules; the only quantitative way to evaluate the chain properties is in terms of thermal averages of observables such as $\langle x \rangle / L$ and *Wr*.

As the force is increased, the plectonemic supercoil progressively unwinds to create extended DNA; for intermediate extensions (e.g., near 1 pN for $\sigma = 0.05$), a "mixed state" of plectonemic and extended DNA is obtained, in accord with analytical theory (Marko and Siggia, 1995b; Marko, 1997). When a large enough force is applied to fully convert the plectonemic DNA to extended DNA, the writhe is essentially entirely converted to twist, and the force-distance behavior reverts to that of untwisted ($\sigma = 0$) DNA. The rapid drop-off of *Wr* for $\sigma = 0.03$ and 0.05 (Fig. 3) thus corresponds to $\langle x \rangle / L$ values (Fig. 2) between the low-force limit and the force-distance curve for $\sigma = 0$.

In all of our simulations with $\sigma > 0.01$, it is essential that we continually check (via computation of the Alexander polynomial; Frank-Kamenetskii et al., 1975) that MC moves do not knot the chain. A transition to a knotted state is, of course, physically forbidden in the kind of twisting-pulling experiment that we have in mind. However, it is interesting to note what happens if one does not check for knotting, but rather fixes only the linking number of the chain. Fig. 5 shows a typical chain conformation that results after equilibration at $\sigma = 0.05$ and $f = 0.2$ pN (the conditions used to generate Fig. 4) if knot checking is not done: tight chiral knots with a high *Wr* and slightly extended ends were obtained. Thus plectonemically interwound unknotted

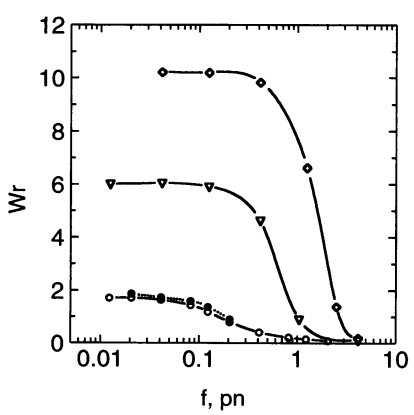

FIGURE 3 Changing of DNA *Wr* versus force. Simulations for $\sigma = 0.01$ (○, ●), 0.03 (▽), and 0.05 (◇) correspond to a monovalent salt concentration of 200 mM. Open symbols indicate results for chains of 10 Kuhn segments (corresponding to 1000-nm or 3-kb DNAs); black circles indicate results for 20 Kuhn segment chains. For $\sigma > 0.03$, *Wr* drops abruptly when force exceeds the threshold for conversion of plectonemic to extended DNA.

FIGURE 4 Simulated conformation of the DNA model for $\sigma = 0.05$, $f =$ 0.2 pN, and 200 mM concentration of monovalent salt. The molecule is nearly entirely plectonemically interwound: the applied force is insufficient to convert the supercoil into extended DNA.

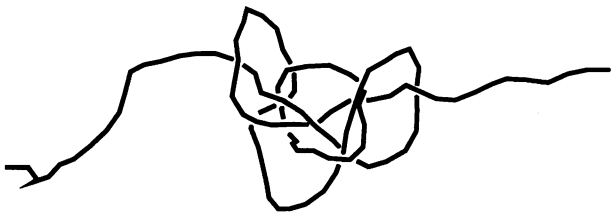

FIGURE 5 Simulated conformation of the model chain for $\sigma = 0.05, f = 0.2$ pN, and 200 mM concentration of monovalent salt (same parameters as Fig. 4), but with the knot type equilibrated (see text). The conformation corresponds to a tight chiral knot with a high *Wr*, and its extension is larger than that of Fig. 4. *Wr* of this conformation is equal to 13.68, which is very close to the value of *Lk* (14) used in this simulation run.

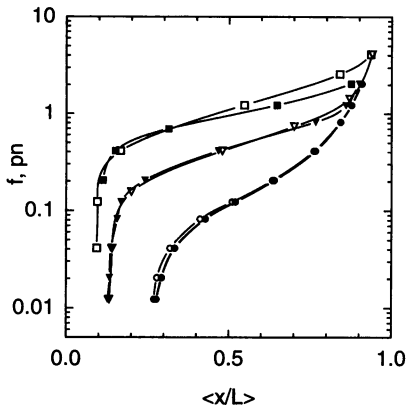

FIGURE 6 Dependence of the simulated force-extension functions on ionic conditions. The DNA effective diameter (hard-core interactions) corresponded to 200 mM (○, □, ▽) and 20 mM (●, ■, ▼) concentrations of monovalent salt. Force-extension dependencies were simulated for σ of 0.01 (○, ●), 0.03 (▽, ▼), and 0.05 (□, ■).

conformations are not the equilibrium states of DNAs with fixed linking number under tension. The equilibrium conformations are knotted. Perhaps these knotted supercoiled conformations of closed circular DNA can be obtained after simultaneous action by two topoisomerases: DNA gyrase, which introduces negative supercoiling into the DNA, and some other topo II enzyme that causes topological relaxation (such a combination of enzymes has been implicated in plasmid segregation in *Escherichia coli*; Zechiedrich and Cozzarelli, 1995).

Effect of reduced ionic strength

Experiments on DNA in vitro are often done at ionic strengths below those encountered physiologically; we now examine the effects of reduced ionic strength. To describe a univalent ionic strength of 20 mM, the effective hard-core diameter must be increased to 11 nm (see Vologodskii and Cozzarelli, 1994b, for a review). An ionic strength of 20 mM is not yet so low that there is appreciable stiffening of the double helix due to electrostatic self-repulsion (this occurs for ionic strengths less than 10 mM; Hagerman, 1988; Vologodskii, 1994; Marko and Siggia, 1995b); we therefore used the same values for bending persistence length and twist persistence length as we used for high ion concentration.

Force versus extension data for 20 mM salt are indicated by the filled symbols in Fig. 6; for comparison, the 200 mM results of the previous subsection are shown with open symbols. For $\sigma = 0.01$ and 0.03, the two data sets are nearly identical: there is nearly no effect of the increase in hard-core diameter. A similar result has been obtained for closed circular DNA with these linkages and hard-core sizes, and it is due to an important entropic effect. For $\sigma < 0.03$, DNA is in a chiral random coil conformation or is rather loosely supercoiled. In the chiral random coil case, close encounters of duplexes are rare enough that they do not affect the chain elasticity; in the case of loose supercoiling, the duplexes tend to stay far apart (>20 nm for $\sigma < 0.03$) to gain conformational entropy (Vologodskii and Cozzarelli, 1994a; Marko and Siggia, 1995a). Thus the increase in hard-core radius does not crucially affect the chain conformations, or therefore the chain elasticity.

For larger $\sigma = 0.05$, the writhe is forced to be so large that the duplexes are driven together closely enough that the differences between the hard-core diameters for 20 mM and 200 mM lead to a slight difference in the force-distance curves at high extensions: at a given extension, the 200 mM force is larger than that for 20 mM, for extensions $\langle x \rangle / L > 0.3$. At higher ionic strength, the duplexes can be more tightly juxtaposed, so the supercoiling free energy is lower (Vologodskii et al., 1992; Marko and Siggia, 1995a). Therefore more work must be done at high ionic strength to convert the plectonemic supercoils to extended DNA, leading to an increase in the force required to obtain a certain extension relative to that for low ionic strength. Analytical calculations for a similar range of ionic strength indicate effects of about the same magnitude as reported here (Marko, 1997). At forces high enough to fully extend the DNA, the hard-core diameter is immaterial, and thus the force-distance curves all eventually collapse to the result for the ideal wormlike chain.

Fig. 7 shows a representative conformation at 20 mM ionic strength, for $\sigma = 0.05$ and $f = 0.2$ pN. At this force, the molecule is only slightly extended and is nearly entirely plectonemically supercoiled. Comparison with Fig. 4, which shows a conformation for the same linkage and force for 200 mM salt, reveals that the larger hard-core diameter forces the supercoil size to increase (note that there are fewer crossings in Fig. 7 than in Fig. 4). For lower σ there are essentially no differences in the conformations at 200 mM and 20 mM ionic strength.

Effect of very high torsional stress

The previous subsection considered linkages in the range $\sigma = 0$ to 0.05. This range (for $|\sigma|$) is roughly that encountered physiologically and is roughly the linkage range that can be accessed using enzymes. Larger $|\sigma|$ may be obtained in micromanipulation experiments; indeed, Strick et al.

FIGURE 7 Simulated conformation of the model chain for $\sigma = 0.05, f = 0.2$ pN, and 20 mM concentration of monovalent salt. Compared with Fig. 4, the decreased ionic strength leads to a less tightly interwound supercoil because of the increased hard-core diameter.

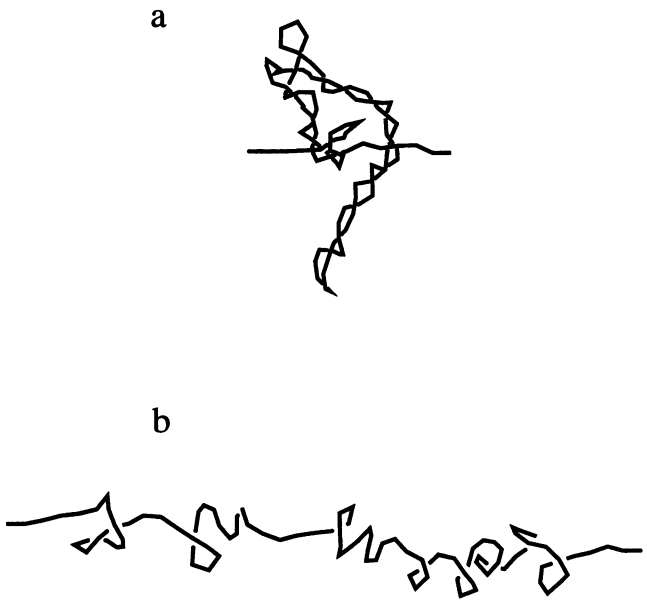

FIGURE 8 Simulated conformation of the model chain under high torsional stress. Conformations correspond to $\sigma = 0.102$, $f = 2$ pN, and monovalent ion concentrations of 200 mM (*a*) and 20 mM (*b*). The chain is tightly plectonemically supercoiled and nearly unextended at high ionic strength; at low ion concentration the chain has a series of tight helical turns along its length, and it is highly extended. The increased hard-core diameter at low ionic strength disfavors tight plectonemic winding in favor of an extended supercoil configuration.

(1996) report force versus distance for DNAs with linkages up to $\sigma = 0.102$. At these large values of σ, supercoiling will be very tight, and we can expect strong ionic strength effects.

Large twists and tensions can potentially change the DNA secondary structure (Cluzel et al., 1996; Smith et al., 1996), and in fact Strick et al. (1996) have observed abrupt changes in extension suggestive of structural transitions of the double helix. Furthermore, we can expect differences between positive and negative σ due to the intrinsic handedness of the double helix; this also has been observed by Strick et al. We have not yet considered such effects in our MC simulations; here we report results for our simple harmonic-twist-energy model as a first step toward understanding the large-σ behavior.

Fig. 8 shows representative conformations for $\sigma = 0.102$ and $f = 2$ pN, for 200 mM and 20 mM ionic strength. In the high-ionic-strength case (Fig. 8 *a*), the molecule is nearly fully plectonemically supercoiled and is almost unextended. Although the supercoils are very tight, the superhelix axis continues to undergo thermal bending (and, occasionally, branching) fluctuations.

At low ionic strength (Fig. 8 *b*), the conformations are totally different: they are highly extended, following the trend observed for $\sigma = 0.05$ of lower ionic strength leading to a more easily extended chain. Remarkably, the low-ionic-strength conformation consists of a series of tight structures reminiscent of the tips of plectonemes. Apparently the tight turns are more favorable than plectonemic interwinding for 20 mM, presumably because of the relatively large hard-core diameter. At lower forces, the chain folds into a plectonemic supercoil with the same handedness as that of Fig. 8 *a*, but with tight turns such as those of Fig. 8 *b* along it.

COMPARISON OF THEORY AND EXPERIMENT

Global comparison

Direct comparison of the simulations with the results of Strick et al. (1996) in the hope of obtaining an estimate for the twist rigidity of DNA was one of the goals of our work. One should keep in mind during the comparison that the experimental results were obtained for λ-DNA that is 50 kb in length and that the simulations correspond to 3-kb DNA. Thus a much smaller wall repulsion effect is expected experimentally. This difference must cause a discrepancy between simulation and experimental results for small extensions, $\langle x \rangle / L < 0.3$. We have compared the $\sigma > 0$ experimental results to our theory because the overwound double helix is less prone to local structural transitions than the underwound one and thus provides a larger range of σ where our model can accurately describe the experimental data. For $|\sigma|$ up to 0.031, Strick et al. (1996) found almost no effect of the sign of σ over the range of forces studied, indicating that our harmonic twist energy approximation is likely applicable in that range for negatively supercoiled DNA as well.

Fig. 9 shows the experimental and simulated force versus extension for the values of σ and ionic conditions used by Strick et al. (1996). The $\sigma = 0$ experimental result (*open circles*) agrees well with the result for the ideal infinite wormlike chain over most of the force range, and agrees with previous experiments on torsionally unconstrained chains (Bustamante et al., 1994). For $\sigma = 0.01$ (*inverted triangles*) the calculated force is systematically slightly below that obtained experimentally over most of the force range. This may reflect the possibility that the twist persistence length is larger than the 75 nm value assumed in the

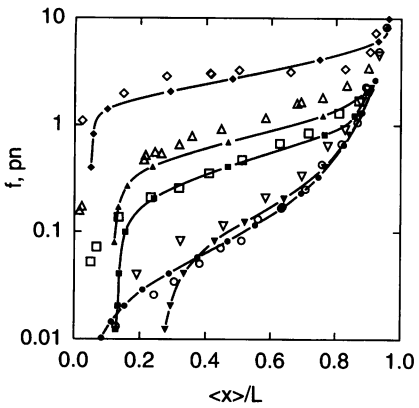

FIGURE 9 Comparison of simulation results for force versus extension to experimental data. The data of Strick et al. (1996) are shown by open symbols and results simulations by filled symbols for $\sigma = 0$ (○, ●), 0.01 (▽, ▼), 0.031 (□, ■), 0.043 (△, ▲), and 0.102 (◇, ◆). Calculations corresponded to a monovalent ion concentration of 20 mM, the ionic condition used by Strick et al. (1996). Filled circles indicate the infinite ideal wormlike chain result (Vologodskii, 1994; Marko and Siggia, 1995b); other filled symbols show MC data. Finite chain effects lead to disagreements between MC and experiment for forces below 0.1 pN; thus theory and experiment should be compared for $\langle x \rangle/L > 0.3$.

MC calculations, although to match the experimental data precisely in this case would require a larger increase in this parameter than would seem reasonable when all of the data are considered (see below).

For $\sigma = 0.031$ (*squares*), MC and experimental results are in excellent quantitative agreement over most of the range of extensions. For $\sigma = 0.043$ (*triangles*), the MC force for a given extension is again slightly below that obtained in experiment. Finally, for large σ (= 0.102), the MC calculation underestimates the force for low extensions and overestimates it for high extensions. Given how large σ is in this last case, it is remarkable how well theory agrees with experiment. Overall, with no adjustment of the parameters, theory and experiment are in quite good agreement over a large range of σ and force.

Twist persistence length

The parameter that is least well known for our DNA model is the twist rigidity C. Previous measurements of C have been based on fluorescence depolarization dynamics (Barkley and Zimm, 1979; Thomas et al., 1980; Shibata et al., 1985; Wu et al., 1991), cyclization rates for linear DNA (Shore and Baldwin, 1983a; Levene and Crothers, 1986; Taylor and Hagerman, 1990), and equilibrium topoisomer distributions (Vologodskii et al., 1979; Shore and Baldwin, 1983b; Horowitz and Wang, 1984; Klenin et al., 1989). Discrepancies remain between the results of these measurements, likely because of the fact that the first type of experiment requires a detailed model of not only static fluctuations, but dynamics as well. By contrast, measurement of supercoil free energies in equilibrium avoids the problem of understanding dynamics, but like fluorescence depolarization and cyclization experiments, relies on spontaneous thermal fluctuations and can only study $|\sigma| < 0.02$. The experiment of Strick et al. (1996) provides a thermodynamic measurement of the response of a DNA to force and twist over a far greater range of $|\sigma|$. Thus we have tried to fit theory to experiment by the adjustment of C.

For $\sigma = 0$, there is of course no effect of C on the chain elasticity. For $\sigma = 0.01$, we have only a small effect of an increase in C on the MC force versus extension. A larger value of C would cause theory to systematically overestimate the experimental force for given extension for all of the larger σ, so we decided not to try to fit C to the $\sigma = 0.01$ data. This might be done once more experimental data are available, and after MC computations become possible for much longer chains, so as to fully discount the possibility of finite-chain effects for the highly disordered chiral random coil case.

Fig. 10 shows MC results for $\sigma = 0.031$ for $C/kT = 50$ nm, 75 nm, and 100 nm, and the corresponding experimental data. One can observe that the change from $C/kT = 50$ nm to 100 nm translates into a rise in the force of a factor of ~2 near $\langle x \rangle/L = 0.5$. The agreement for $C/kT = 75$ nm is quite good; $C/kT = 100$ nm causes the force curve to be too high, whereas $C/kT = 50$ nm leads to forces that are too low. Thus we are led to the preliminary conclusion that the direct force-distance measurement is consistent with $C/kT = 75$ nm, with an uncertainty on the order of 15 nm, in good agreement with previous determinations based on supercoil free energy (Vologodskii et al., 1979).

CONCLUSION

This study has examined the elasticity of twisted DNA, using a wormlike chain model with harmonic twist energy. We have found good agreement with recent experiments of Strick et al. (1996), using an accepted value for the bending persistence length and a twist persistence length of 75 nm, corresponding to a twist rigidity of $C = 3.0 \times 10^{-19}$

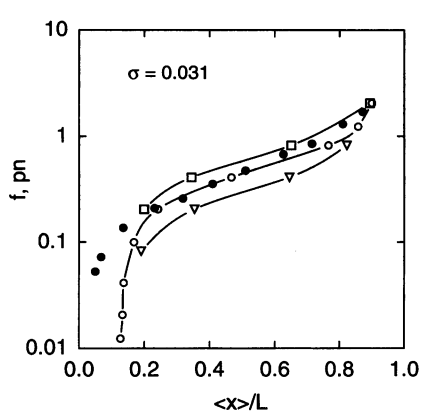

FIGURE 10 Effect of twist persistence length C/kT on force-extension dependence. Simulated results for $\sigma = 0.031$ and $C/kT = 75$ nm (○), $C/kT = 100$ nm (□), and $C/kT = 50$ nm (▽) are shown together with the experimental data of Strick et al. (1996) (●).

erg · cm. For low superhelix densities ($\sigma < 0.03$) the DNA is not plectonemically supercoiled at low forces and has a smooth force-distance behavior reminiscent of the wormlike chain entropic elasticity. For larger superhelix densities ($\sigma > 0.03$), the DNA is plectonemically supercoiled at low forces, and a finite force threshold must be overcome to extend it. Extension of the DNA reduces its writhe; this reduction becomes more abrupt as σ is increased.

Our results showed that comparison of such experimental data with computer simulation can be used to measure DNA torsional rigidity because the force-extension dependencies are rather sensitive to this parameter. At the moment we are not able to obtain perfect agreement between experimental data and simulation results for σ of 0.01, 0.031, and 0.043 for any value of C. From the current data we conclude that C is bigger than 3×10^{-19} erg · cm; restricting our attention to the $\sigma = 0.031$ data, we estimate that $C/kT = 75$ nm, with an uncertainty of 15 nm. More precise determination of C by using larger computer simulations would be feasible once more experimental data are available. More experimental data might also allow effects beyond the present model to be considered, such as the progressive lengthening of the double helix as it is untwisted, and nonlinearity of the twist elasticity.

An essential feature of the experimental data that we have not addressed is the appearance of force "plateaus," which have been proposed to be due to changes in DNA structure by torsional stress. These plateaus dominate the experimental data for $\sigma < -0.031$ and for $\sigma > 0.1$. The present model could be modified to take into account abrupt twist changes (e.g., formation of Z-DNA); however, large displacements of the complementary strands (e.g., formation of cruciforms or open regions) can only be studied by using a model that explicitly keeps track of both strands.

The authors thank D. Bensimon, V. Croquette, and T. Strick for many helpful discussions and for providing their experimental data.

AV acknowledges the support of the Center for Studies in Physics and Biology of the Rockefeller University during early 1996; JM thanks the Meyer Foundation and Rockefeller University for supporting this research.

REFERENCES

Barkley, M. D., and B. H. Zimm. 1979. Theory of twisting and bending of chain macromolecules; analysis of the fluorescence depolarization of DNA. *J. Chem. Phys.* 70:2991–3007.

Brian, A. A., H. L. Frisch, and L. S. Lerman. 1981. Thermodynamics and equilibrium sedimentation analysis of the close approach of DNA molecules and a molecular ordering transition. *Biopolymers.* 20:1305–1328.

Bustamante, C., J. F. Marko, E. D. Siggia, and S. Smith. 1994. Entropic elasticity of lambda-phage DNA. *Science.* 265:1599–1600.

Cluzel, P., A. Lebrun, C. Heller, R. Lavery, J. L. Viovy, D. Chatenay, and F. Caron. 1996. DNA: an extensible molecule. *Science.* 271:792–794.

Crothers, D. M., J. Drak, J. D. Kahn, and S. D. Levene. 1992. DNA bending, flexibility, and helical repeat by cyclization kinetics. *Methods Enzymol.* 212:3–29.

de Gennes, P. G. 1979. Scaling Concepts in Polymer Physics. Cornell University Press, Ithaca, NY.

Frank-Kamenetskii, M. D., A. V. Lukashin, V. V. Anshelevich, and A. V. Vologodskii. 1985. Torsional and bending rigidity of the double helix from data on small DNA rings. *J. Biomol. Struct. Dyn.* 2:1005–1012.

Frank-Kamenetskii, M. D., A. V. Lukashin, and M. D. Vologodskii. 1975. Statistical mechanics and topology of polymer chains. *Nature.* 258: 398–402.

Fuller, F. B. 1971. The writhing number of a space curve. *Proc. Natl. Acad. Sci. USA.* 68:815–819.

Gebe, J. A., S. A. Allison, J. B. Clendenning, and J. M. Schurr. 1995. Monte Carlo simulations of supercoiling free energies for unknotted and trefoil knotted DNAs. *Biophys. J.* 68:619–633.

Gebe, J. A., J. J. Delrow, P. J. Heath, B. S. Fujimoto, D. W. Stewart, and J. M. Schurr. 1996. Effects of Na^+ and Mg^{2+} on the structures of supercoiled DNAs: comparison of simulations with experiments. *J. Mol. Biol.* 262:105–128.

Hagerman, P. J. 1988. Flexibility of DNA. *Annu. Rev. Biophys. Biophys. Chem.* 17:265–286.

Hao, M.-H., and W. K. Olson. 1989. Global equilibrium configurations of supercoiled DNA. *Macromolecules.* 22:3292–3303.

Horowitz, D. S., and J. C. Wang. 1984. Torsional rigidity of DNA and length dependence of the free energy of DNA supercoiling. *J. Mol. Biol.* 173:75–91.

Katritch, V., and A. Vologodskii. 1997. The effect of intrinsic curvature on conformational properties of circular DNA. *Biophys. J.* 72:1070–1079.

Klenin, K. V., A. V. Vologodskii, V. V. Anshelevich, A. M. Dykhne, and M. D. Frank-Kamenetskii. 1991. Computer simulation of DNA supercoiling. *J. Mol. Biol.* 217:413–419.

Klenin, K. V., A. V. Vologodskii, V. V. Anshelevich, V. Y. Klisko, A. M. Dykhne, and M. D. Frank-Kamenetskii. 1989. Variance of writhe for wormlike DNA rings with excluded volume. *J. Biomol. Struct. Dyn.* 6:707–714.

Levene, S. D., and D. M. Crothers. 1986. Ring closure probabilities for DNA fragments by Monte Carlo simulation. *J. Mol. Biol.* 189:61–72.

Marko, J. F. 1997. Supercoiled and braided DNA under tension. *Phys. Rev. E.* 55:1758–1772.

Marko, J. F., and E. D. Siggia. 1994. Fluctuations and supercoiling of DNA. *Science.* 265:506–508.

Marko, J. F., and E. D. Siggia. 1995a. Statistical mechanics of supercoiled DNA. *Phys. Rev. E.* 52:2912–2938.

Marko, J. F., and E. D. Siggia. 1995b. Stretching DNA. *Macromolecules.* 28:8759–8770.

Metropolis, N., A. W. Rosenbluth, M. N. Rosenbluth, A. H. Teller, and E. Teller. 1953. Equation of state calculations by fast computing machines. *J. Chem. Phys.* 21:1087–1092.

Perkins, T. T., S. R. Quake, D. E. Smith, and S. Chu. 1994. Relaxation of a single DNA molecule observed by optical microscopy. *Science.* 264: 822–826.

Perkins, T. T., D. E. Smith, R. G. Larson, and S. Chu. 1995. Stretching of a single tethered polymer in a uniform flow. *Science.* 268:83–86.

Rybenkov, V. V., N. R. Cozzarelli, and A. V. Vologodskii. 1993. Probability of DNA knotting and the effective diameter of the DNA double helix. *Proc. Natl. Acad. Sci. USA.* 90:5307–5311.

Shaw, S. Y., and J. C. Wang. 1993. Knotting of a DNA chain during ring closure. *Science.* 260:533–536.

Shibata, J. M., B. S. Fujimoto, and J. M. Schurr. 1985. Rotational dynamics of DNA from 10e-10 to 10e-5 seconds: comparison theory with optical experiments. *Biopolymers.* 24:1909–1930.

Shore, D., and R. L. Baldwin. 1983a. Energetics of DNA twisting. I. Relation between twist and cyclization probability. *J. Mol. Biol.* 170: 957–981.

Shore, D., and R. L. Baldwin. 1983b. Energetics of DNA twisting. II. Topoisomer analysis. *J. Mol. Biol.* 170:983–1007.

Smith, S. B., Y. Cui, and C. Bustamante. 1996. Overstretching B-DNA: the elastic response of individual double-stranded and single-stranded DNA molecules. *Science.* 271:795–799.

Smith, S. B., L. Finzi, and C. Bustamante. 1992. Direct mechanical measurements of the elasticity of single DNA molecules by using magnetic beads. *Science.* 258:1122–1126.

Stigter, D. 1977. Interactions of highly charged colloidal cylinders with applications to double-stranded DNA. *Biopolymers.* 16:1435–1448.

Strick, T. R., J. F. Allemand, D. Bensimon, A. Bensimon, and V. Croquette. 1996. The elasticity of a single supercoiled DNA molecule. *Science.* 271:1835–1837.

Tan, R. K. Z., and S. C. Harvey. 1989. Molecular mechanics model of supercoiled DNA. *J. Mol. Biol.* 205:573–591.

Taylor, W. H., and P. J. Hagerman. 1990. Application of the method of phage T4 DNA ligase-catalyzed ring-closure to the study of DNA structure. II. NaCl-dependence of DNA flexibility and helical repeat. *J. Mol. Biol.* 212:363–376.

Thomas, J. C., S. A. Allison, C. J. Appelof, and J. M. Schurr. 1980. Torsional dynamics and depolarization of fluorescence of linear macromolecules. II. Flourescence polarization anisotropy measurements on a clean viral f29 DNA. *Biophys. Chem.* 12:177–188.

Vologodskii, A. V. 1992. Topology and Physics of Circular DNA. CRC Press, Boca Raton, FL.

Vologodskii, A. V. 1994. DNA extension under the action of an external force. *Macromolecules.* 27:5623–5625.

Vologodskii, A. V., V. V. Anshelevich, A. V. Lukashin, and M. D. Frank-Kamenetskii. 1979. Statistical mechanics of supercoils and the torsional stiffness of the DNA. *Nature.* 280:294–298.

Vologodskii, A. V., and N. R. Cozzarelli. 1993. Monte Carlo analysis of the conformation of DNA catenanes. *J. Mol. Biol.* 232:1130–1140.

Vologodskii, A. V., and N. R. Cozzarelli. 1994a. Conformational and thermodynamic properties of supercoiled DNA. *Annu. Rev. Biophys. Biomol. Struct.* 23:609–643.

Vologodskii, A. V., and N. R. Cozzarelli. 1994b. Supercoiling, knotting, looping, and other large-scale conformational properties of DNA. *Curr. Opin. Struct. Biol.* 4:372–375.

Vologodskii, A. V., S. D. Levene, K. V. Klenin, M. D. Frank-Kamenetskii, and N. R. Cozzarelli. 1992. Conformational and thermodynamic properties of supercoiled DNA. *J. Mol. Biol.* 227:1224–1243.

Vologodskii, A. V., A. V. Lukashin, V. V. Anshelevich, and M. D. Frank-Kamenetskii. 1979. Fluctuations in superhelical DNA. *Nucleic Acids Res.* 6:967–982.

Vologodskii, A. V., A. V. Lukashin, M. D. Frank-Kamenetskii, and V. V. Anshelevich. 1974. Problem of knots in statistical mechanics of polymer chains. *Sov. Phys. JETP.* 39:1059–1063.

White, J. H. 1969. Self-linking and the Gauss integral in higher dimensions. *Am. J. Math.* 91:693–728.

White, J. H. 1989. An introduction to the geometry and topology of DNA structure. *In* Mathematical Methods for DNA Sequences. M. S. Waterman, editor. CRC Press, Boca Raton, FL.

Wu, P. G., B. S. Fujimoto, L. Song, and J. M. Schurr. 1991. Effect of ethidium on the torsion constants of linear and supercoiled DNAs. *Biophys. Chem.* 41:217–236.

Zechiedrich, E. L., and N. R. Cozzarelli. 1995. Roles of topoisomerase IV and DNA gyrase in DNA unlinking during replication in *Escherichia coli. Genes Dev.* 9:2859–2869.